Determination of Selenium(IV) at a Microfabricated Gold Ultramicroelectrode Array Using Square Wave Anodic Stripping Voltammetry

Sandie H. Tan and *Samuel P. Kounaves**

Department of Chemistry, Tufts University, Medford, Massachusetts 02155, USA

Received: January 12, 1998
Final version: February 27, 1998

Abstract
The voltammetric determination of selenium(IV) using a microfabricated array of gold ultramicroelectrodes (Au UMEs) is presented. The array of Au UMEs in conjunction with square wave anodic stripping voltammetry shows a rapid, sensitive and reproducible response for selenium. Using an array of UMEs overcomes the inherent disadvantage of measuring the very low current signals present when using a single UME. The experimental parameters that affect the response of selenium: deposition potential, selection of the electrolyte solution, SW frequency, and deposition time were investigated. The Se redox reaction appears to be kinetically faster and more reversible at the Au UME array than at Au macroelectrode or single Au UME. Calibration plots are given for solutions containing 0–100 ppb and 100–500 ppb. The limit of detection is calculated to be 0.42 ppb. The relative standard deviation at 50 ppb is 4.5 % for 10 runs.

Keywords: Selenium, Square wave anodic stripping voltammetry, Gold ultramicroelectrode arrays, In-situ analysis, Microlithographic fabrication

1. Introduction

In recent years, trace analysis of selenium has received considerable attention due mainly to this metalloid's significant roles in biological, environmental, and industrial processes [1, 2]. There is a very narrow concentration range where it functions, as an essential nutrient but in excess rapidly becomes very toxic to a wide variety of organisms [2–4]. The release of increasing amounts of selenium into the environment, and especially the effects of the Se^{4+} species on the ecosystem, has prompted the development of sensors for field portable technologies, which are capable of rapid on-site analysis. There are currently several laboratory-based analytical techniques used to analyze for Se^{4+} in various matrices. These include atomic absorption spectrometry [5–7], atomic fluorescence spectrometry [8, 9], high pressure liquid chromatography [10, 11], gas chromatography [12, 13], and flow injection analysis [14, 15]. However most of these techniques are either not easily amendable to on-site analysis and/or do not provide the sensitivity or limits of detection required.

Several electroanalytical techniques, especially stripping voltammetry, not only offer the advantages of high sensitivity and low cost, but due to simple instrumentation, can be easily utilized for on-site analysis. In the environment, inorganic selenium exists in various oxidation states. These are elemental selenium (Se^0), selenide (Se^{2-}), selenite (Se^{4+}), and selenate (Se^{6+}). The Se^{4+} and Se^{6+} forms are both commonly found in natural waters [16], but of the two species, Se^{4+} is the more highly toxic. This is fortunate in terms of electroanalysis, since Se^{4+} is the only electroactive form and can be easily analyzed by stripping voltammetry. In order for total Se to be determined, the Se^{6+} must first be reduced to Se^{4+}.

In the past, several voltammetric stripping techniques have been extensively applied in studying selenium in various aqueous matrices. These have included adsorptive [17–19], cathodic [20–23], and anodic [24], stripping voltammetry. Andrews and Johnson [25] in 1975 first demonstrated the use of a gold substrate for selenium detection using linear scan anodic stripping voltammetry (LSASV). Since then, several other studies have successfully used gold, sometimes with polymer coatings, as a substrate for stripping voltammetric flow injection analysis [26–28].

All of the previous ASV analyses for selenium have used either a large macroelectrode or a single disk ultramicroelectrode (UME). However, UMEs are especially advantageous for environmental analysis because they offer not only the ability of being used in high-resistance natural waters, but more importantly, with lower concentrations of electrolytes when they are an unavoidable part of the analytical procedure. Solution samples need not be stirred due to the high mass transfer present at ultramicroelectrodes. The properties of UMEs have been well documented [29]. Recently, Hrehocik et al. [30] undertook a comparative study of several electrode geometries and came to the conclusion that single UMEs, were about eight times more sensitive than other macroelectrode geometries for analysis of Se by ASV. However, they also noted that because of the small size, and thus small currents, the LOD was limited by instrumental inability to detect such low current levels. To overcome the low current problem one may combine individual UMEs into an array, thus multiplying the current. We have previously shown that an ideal way to accomplish this is by using microlithographic fabrication technology with standard silicon wafers as the substrate on which to pattern the desired metal UME array [31, 32]. The combination of this technology with the fast and sensitive technique of square wave anodic stripping voltammetry (SWASV) [33] has recently been shown to be advantageous for on-site and in-situ environmental detection of several metals [34]. The adaptation of this technology to ASV of Se^0/Se^{4+} on a gold UME array could provide a substantial improvement for on-site rapid analysis for selenium. This article describes the use of microlithographically fabricated arrays of gold ultramicroelectrodes in conjunction with SWASV for the detection of Se^{4+} in aqueous solutions.

2. Experimental

2.1. Electrochemical Apparatus and Parameters

Cyclic voltammetry, chronoamperometry, and SWASV were performed with an EG&G PAR Model 263 and Model 273 potentiostat/galvanostat (EG&G PAR, Princeton, NJ) interfaced to

  1040-0397/98/0605-0364 $ 17.50+.50/0

a DEC p420-SX microcomputer and using the Model 270 software (EG&G PAR). All voltammetric experiments were performed using a three electrode system consisting of a gold ultramicroelectrode array (Au UMEA) as the working electrode, a Ag/AgCl (saturated)/NaCl(3M) reference electrode (Bioanalytical Systems, West Lafayette, IN, USA) against which all potentials were measured, and a Pt wire counter electrode.

The SWASV conditions used unless otherwise noted were, initial potential: −200 mV, final potential: 1000–1050 mV, pulse height: 25 mV, step height: 2 mV and frequency: 180 Hz. The solutions were neither purged nor stirred during deposition. The deposition times varied with the experiments performed.

2.2. Reagents

All solutions were prepared with 18 MΩ-cm deionized water from a Barnstead Nanopure System (Barnstead Co., Debuque IA). Selenium dioxide (SeO_2) was purchased from Aldrich (99.999 %). The SeO_2 was dissolved in 0.05M H_2SO_4 (99.999 %, Fisher Scientific) to give a stock metal solution of 1000 ppm Se^{4+} and dilutions were made to give the appropriate calibration standards. All other solutions were made from ACS reagent grade chemicals. Experiments were carried out at room temperature (23 ± 3 °C). Glassware for all experiments was kept in 8 M HNO_3 for 1 week and rinsed thoroughly with 18 MΩ cm deionized water before use. Unless otherwise indicated, the electrolyte consisted of either 0.05 M or 0.005 M H_2SO_4.

2.3. Microlithographic Fabrication of the Au UME Array

The Au UMEA sensors were custom fabricated for us at the IBM Watson Research Center, CSS Microfabrication Laboratory, Yorktown Heights, NY. A five-inch silicon wafer was thermally oxidized to grow a layer of SiO_2. On top of this were successively deposited by electron beam evaporation, a titanium layer (100 Å), a gold layer (5000 Å), and another titanium layer (100 Å). A final layer of silicon dioxide (5000 Å) was reactively sputter deposited to form an insulating layer. The silicon dioxide layer was then photolithographically stenciled with the desired array design and the appropriate areas removed by reactive ion etching. An argon ion beam was the used to further etch the titanium layer and expose the gold UMEs. A gold pad was also exposed to allow for a ball-bonded electrical connection between the UME array and a pad on the printed circuit (PC) carrier board. Each diced chip, measuring 3.1 mm × 3.4 mm, contains an array of 564 interconnected disk shaped Au UMEs. Each UME measures 12 μm in diameter and is 66 μm (center-to-center) from its nearest neighbor.

The chip was then glued onto the custom designed PC board (CFC, Waltham, MA) with epoxy (Epo-Tek 905, Epoxy Technology Inc. Billerica, MA). A single length of 1.25 μm gold wire (99.99 %, Williams Advanced Materials, Buffalo, NY) was used to attach the chip to the PC board. The gold bonding wire was then encased using a special epoxy (proprietary formulation, Orion Research Inc. Beverly, MA) which was cured at 50 °C for three hours.

2.4. Cleaning and Conditioning of the Au UME Array

All the Au UME arrays were initially electrochemically cleaned by scanning the potential between 600 mV and 1500 mV for 5 cycles. Before any experiments were performed with an individual Au UME array, it was preconditioned at least once a day by being held for 30 s at 2000 mV. In addition, before each analysis the array was further conditioned at a potential of 1300 or 1400 mV for 30 s to prevent any memory effects from the previous ASV run.

3. Results and Discussion

3.1. Evaluation of the UME Arrays

Before the arrays were used for analysis of selenium, they were evaluated by obtaining cyclic voltammograms in a solution containing 6×10^{-3} M $K_3(FeCN)_6$ and 1.0 M KNO_3. The behavior of a typical Au UME array for the fastest and slowest scan rates is shown in Figure 1. The scan rates ranged from 1 mV/s to 13 000 mV/s and the applied potential cycled from 450 to 50mV and back to 450mV again. The differences observed in the cyclic voltammograms are due to the change in the diffusion geometry with scan rate. At slow scan rates (1 mV/s) the diffusion layer becomes spherical and attains a steady-state resulting in the observed sigmoidal shape. At higher scan rates (13 000 mV/s) the diffusion layer remains planar and results in a classical CV curve normally seen at a large electrode. The sigmoidal shape of the CV at a scan rate of 1 mV/s indicates that the 66 μm center-to-center separation of the individual UME elements is sufficient to avoid having the individual spherical diffusion volumes coalesce into one larger planar diffusion field. Thus, the collection of UMEs behaves as a single UME.

3.2. Stripping Mechanisms of Selenium

It has been shown in previous work by Andrews and Johnson [25], using linear scan ASV at a large rotating Au-disk electrode in 0.1 M $HClO_4$, that three stripping peaks are observed during the anodic scan after depositing Se on the surface. The origins of these peaks, during the stripping scan, were attributed the three different surroundings or interactions in which Se finds itself on the surface of the electrode. These include: 1) Se deposited on Se to give bulk Se; 2) the reaction of the bulk Se and Au at the Se/Au interface to give a Se-Au intermetallic compound of unknown stoichiometry; and 3) a monolayer of Se directly in contact with the Au electrode surface.

The reaction that we consider of greatest analytical interest, and have focused on in this study, is that of the reduction and stripping of the monolayer of Se at the Au UME array surface. Figure 2

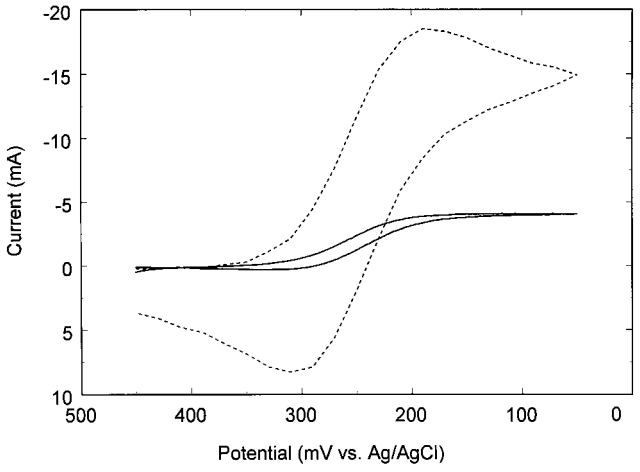

Fig. 1. Cyclic voltammograms of 6×10^{-3} M $K_3(FeCN)_6$ in 1.0 M KNO_3 at a Au UME array showing the curves for only the slowest, 1 mV/s (——), and the fastest, 13 000 mV/s (-----), scan rates.

shows the typical forward (------), reverse (·····), and net (——) SWASV currents for a solution containing 20 ppb Se^{4+} and 0.005 M H_2SO_4. The array was initially conditioned at a potential of 1400 mV for 30 s. The Se^{4+} was then reduced for a deposition time (t_d) of 200 seconds at a potential (E_{dep}) of −200 mV. The potential was then scanned anodically from −200 to +1050 mV. The SW frequency was 180 Hz, with a pulse height of 25 mV, and pulse amplitude of 2 mV. The resulting anodic direction of the reverse current peak can be attributed to the irreversible nature of the deposition reaction. Since the deposition of the Se monolayer occurs at an under potential deposition (UPD) approximately 300 mV anodic of the bulk deposition of Se on Se, the reverse pulse height is insufficient to cause the reduction of all the Se^{4+} back to Se again.

3.3. Optimization of Parameters

3.3.1. Deposition Potential

The effect of deposition potential on stripping peak response was studied by varying the applied E_{dep} and recording a voltammogram at each point. The solution consisted of 100 ppb Se^{4+} in 0.05 M H_2SO_4. The deposition time for all points was 180 s. The initial potential for each SWASV experiment was the same as the deposition potential. The SW frequency was 120 Hz, pulse height: 25 mV, and pulse amplitude: 2 mV. The Au UME array was preconditioned for 30 s at 1300 mV previous to each run. Figure 3 shows a typical plot of the stripping peak current (i_p) as a function of the deposition potential (○). For deposition potentials from 0 to −300 mV a relatively flat diffusion controlled plateau is obtained. For potentials more cathodic than −300 mV the peak currents decrease due to the increasingly competitive production of H_2 at the bare gold surface. At potentials more anodic than 0 mV the peaks decrease and form the expected sigmoidal shape. The solid line in Figure 3 is then calculated for best fit to the polarographic wave equation $E_{app} = E_{½} - (0.059/n)\ \log(i/i_d\text{-}i)$ and gives an $E_{½}$ of approximately 72 mV, a slope of 48 mV, with a correlation coefficient of 0.992. This value of the slope is in contrast with the 420 mV for a single 10 μm UME or 150 mV for a 1.7 mm Au disk electrode that is given in reference [30]. Thus, it would appear that the Au UME arrays described here do not suffer from the same slow electron transfer kinetics ascribed to those. For analytical purposes,

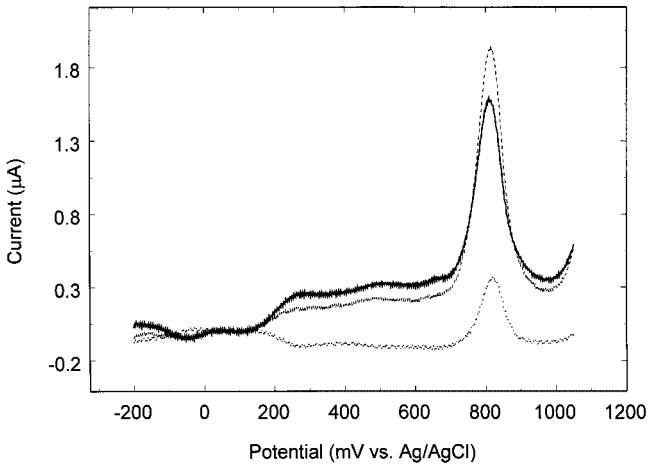

Fig. 2. SW anodic stripping voltammogram of Se^{4+} at a Au UME array showing the forward (-----), reverse (·····), and net (——) currents for a solution containing 20 ppb Se^{4+} in 0.005 M H_2SO_4. Deposition time: 200 s, conditioning potential: 1400 mV, conditioning time: 30 s, initial potential: −200 mV, final potential: 1050 mV, SW frequency: 180 Hz, pulse height: 25 mV, and pulse amplitude: 2 mV.

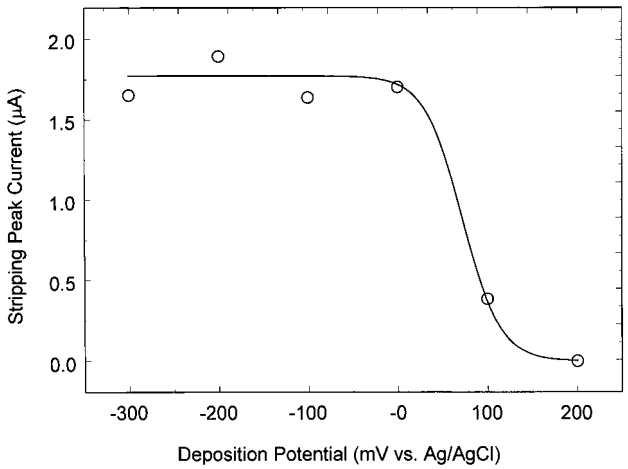

Fig. 3. The current peak response to varying deposition potentials. Solution: 100 ppb Se^{4+} in 0.05 M H_2SO_4. Initial potential: −200 mV, final potential: 1000 mV, frequency 120 Hz, deposition time 180 s. pulse height: 25 mV, conditioning potential: 1300 mV, conditioning time: 30 s. The solid line is the calculated best fit to the polarographic wave equation and gives an $E_{½}$ of 72 mV, a slope of 48 mV, with a correlation coefficient of 0.992.

to assure reasonable selectivity in the presence of other metals and provide maximum mass transfer, it then appears reasonable that the deposition potential should be set approximately between −200 and 0 mV for optimum results.

3.3.2. Selection of Electrolyte

The initial choice of 0.05M H_2SO_4 as the electrolyte was based on two published studies [35, 36]. In both cases H_2SO_4 was recommended as the electrolyte of choice, having been demonstrated that $HClO_4$, HNO_3, and HCl all either suppressed or distorted the ASV peak response. Studies carried in our lab confirmed these results. However, we observed that at concentrations of greater than 0.1 M H_2SO_4 the ASV peak shapes and heights also deteriorated. Decreasing the concentration down to 0.005 M the ASV peak heights increased and reproducibility substantially improved. Thus, for analysis with UME arrays it appears optimum to use this lower concentration.

3.3.3. Effect of Deposition Time

The response of the peak stripping current with increased deposition time (t_d) is important because the peak current at 800 mV (Fig. 2) results from the oxidation of a monolayer of Se at the Au surface. Thus, as the deposition time (or concentration of Se^{4+}) is increased, we should see this peak begin to level off. As can be seen in Figure 4, this is exactly the response observed for a solution containing 20 ppb Se^{4+} in 0.005 M H_2SO_4. For $t_d > 200$ s the peak current substantially tapers off. However, for $t_d > 400$ s it begins to decrease even further. This is not unexpected since, under the influence of the bulk Se, there is most likely an additional loss of the Se monolayer as it dissolves into the Au surface to form a Au-Se intermetallic compound. As will become evident below, the optimum response is obtained with a combination of the appropriate concentration and deposition time.

3.3.4. Effect of SW Frequency

For SWASV, theory indicates that the peak current is proportional to the SW frequency, so, for a typical ASV experiment with a thin mercury film, increasing the SW frequency typically improves the analytical sensitivity [37]. The response is also influenced by both the electronics and the kinetics of the redox system being

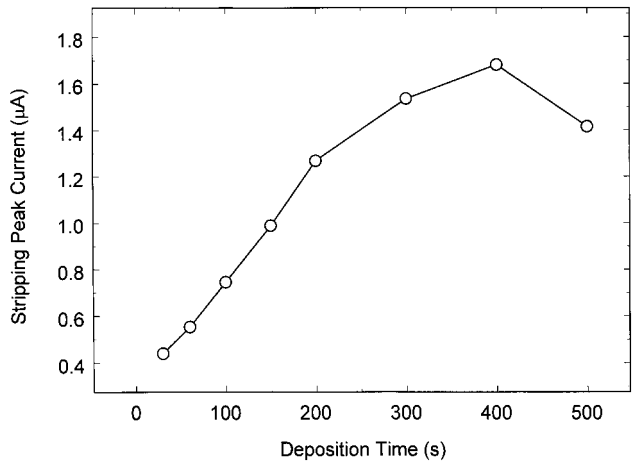

Fig. 4. The current peak response to varying deposition times. Solution: 20 ppb Se^{4+} in 0.005 M H_2SO_4. Experimental conditions are the same as in Figure 2 with the exception of the deposition times.

analyzed. Even though the theory was developed for a metal being reduced into a mercury film, it is interesting to note the peak current response for Se on a solid electrode behaves in accordance with it. The stripping peak current as a function of the SW frequency was plotted for SWASV runs made with a solution containing 100 ppb Se in 0.005 M H_2SO_4, a deposition time of 90 s and other parameters were the same as in Figure 2. As the SW frequency was varied from 15 Hz to 600 Hz the peak current increased linearly. However, at a frequencies greater than about 180 Hz there was an increase in the background current with the peaks becoming increasingly distorted. Thus, we selected 180 Hz as the optimum SW frequency for analysis.

3.4. Calibration Plots

Because the monolayer peak is being used for the analysis, it is difficult to obtain a very large linear dynamic range using only one concentration and/or deposition time. Figure 5 shows calibration plots for $t_d = 200$ s (○) and $t_d = 10$ s (□). As can be seen, for the 200 s plot there is a plateau starting at about a concentration of 100 ppb due to the 'saturation' of the monolayer. For this plot the correlation coefficient for a linear fit was 0.977 and the LOD (3σ) was 0.42 ppb.

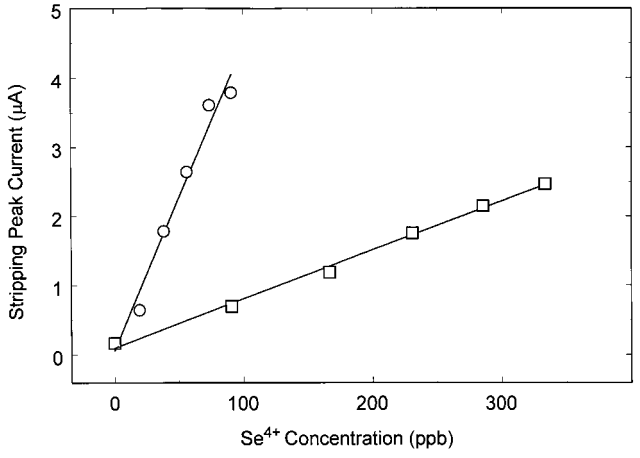

Fig. 5. Calibration plot for 0–100 ppb Se^{4+} with $t_d = 200$ s (○) and for 0–500 ppb Se^{4+} with $t_d = 10$ s (□) in a solution of 0.005 M H_2SO_4. Deposition potential: −200mV, SW frequency: 180 Hz, pulse height: 25 mV, pulse step 2 mV, preconditioned at 1300 mV for 30 s.

In order to extend the linearity it then becomes necessary to decrease the deposition time. For $t_d = 10$ s (□) the linear range can be extended out to 400 ppb. For this case the correlation coefficient was 0.996. The relative standard deviation for 10 consecutive runs was 4.5 % for 50 ppb Se^{4+} solution.

4. Conclusions

The detection of Se^{+4} using SWASV with Au UME arrays has been successfully demonstrated. The optimization of the parameters of this technique allowed for consistent and reproducible results, in particular the use of the array of UMEs, which amplified the current response. UMEs offer advantages that large Au electrodes do not have such as the use of quiescent solutions, high sensitivity and a wider range of linearity. The Se redox reaction appears to be kinetically faster and more reversible at the Au UME array than at Au macroelectrode or single Au UME. Future work is underway to demonstrate the use of these sensors for testing natural samples as a method of providing rapid on-site analysis for selenium.

5. Acknowledgements

This work was supported in part by grants from the National Science Foundation (CHE-9256871) and the Environmental Protection Agency through the Northeast Hazardous Substance Research Center at NJIT. We also wish to thank James Doyle and James Speidell at the IBM Watson Research Center, CSS Microfabrication Laboratory in Yorktown Heights, NY, for the microlithographic fabrication of the UMEA chips.

6. References

[1] S.E. Raptis, G. Kaiser, G. Tolg, Fresnius Z. *Anal Chem.* **1983**, *316*, 105.
[2] T.C. Stadtman, *Science* **1974**, *183*, 915.
[3] S.B. Adeloju, A.M. Bond, M.H. Briggs, H.C. Hughes, *Anal Chem.* **1983**, *55*, 2076.
[4] M.S. Alaejos, C.D. Romero, *Chem. Rev.* **1995**, *95*, 227.
[5] H. Benemariya, H. Robberecht, H. Dellstra, *Sci. Tot. Environ.* **1991**, *105*, 73.
[6] T. Kubota, T. Okutani, *Anal. Chim. Acta* **1997**, *351*, 319.
[7] G. Kaiser, G. Tolg, *Fresenius Z. Anal. Chem.* **1986**, *325*, 32.
[8] S.J. Hill, L. Pitts, P. Worsfold, *J. Anal. Atomic Spectr.* **1995**, *10*, 409.
[9] E.M. Rodriquez Rodriguez, M. Sanz Alaejos, C. Diaz Romero, *Anal. Chim. Acta* **1996**, *334*, 161.
[10] G. Kolb, *Marine Chemistry* **1995**, *48*, 185.
[11] T. Guerin, A. Astruc, M. Astruc, A. Batel, M. Borsier, *Jol. Chromatogr. Sci.* **1997**, *35*, 213.
[12] A.K. Singh, T. White, T. Arendt, Y. Jiang, *Jol. Chromatogr. B* **1997**, *690*, 327.
[13] S. Nielsen, J.J. Sloth, E.H. Hansen, *Analyst* **1996**, *121*, 131.
[14] Z. Ouyang, P. Xu, G. Xiong, Y. Liu, *Talanta* **1986**, *33*, 443.
[15] M.J. Ahmed, C.D. Stalikas, P.G. Veltsistas, S.M. Tzouwara-Karayanni, M. I. Karayannis, *Analyst* **1997**, *122*, 221.
[16] J.E. Conde, M. Sanz Alaejos, *Chem. Rev.* **1997**, *97*, 1979.
[17] J. Wang, C. Sun, *J. Electroanal. Chem.* **1990**, *291*, 59.
[18] L. Chiang, B.D. James, R.J. Magee, *Mikrochim. Acta* **1989**, *II*, 149.
[19] V. Stara, M. Kopanica, *Anal. Chim. Acta* **1988**, *208*, 231.
[20] T.P. Rao, M. Anbu, M.L.P. Reddy, C.S.P. Iyer, A.D. Damodaran, *Anal. Lett.* **1996**, *29*, 2563.
[21] T. Ferri, F. Guidi, R. Morabito, *Electroanalysis* **1994**, *6*, 1087.
[22] T. Ishiyama, T. Tanaka, *Anal. Chem.* **1996**, *68*, 3789.
[23] B. Lange, F. Scholz, *Fresenius J Anal. Chem.* **1997**, *358*, 736.
[24] Z. Yang, Y. He, C. Liu, L. Zhang, *Pedosphere* **1994**, *4*, 181.
[25] R.W. Andrews, D.C. Johnson, *Anal. Chem.* **1975**, *47*, 294.
[26] D.W. Byrce, A. Izquierdo, M.D. Luque de Castro, *Anal. Chim. Acta* **1995**, *308*, 96.
[27] K. McLaughlin, D. Boyd, H. Chi, M. R. Smyth, *Electroanalysis* **1992**, *4*, 689.

[28] Q. Cai, S.B. Khoo, *Anal. Chem.* **1994**, *66*, 4543.
[29] S. Pons, M. Flesichmann, *Anal. Chem.* **1987**, *59*, 1391A.
[30] M.H. Hrehocik, J.S. Lundgren, W.J. Bowyer, *Electroanalysis* **1993**, *5*, 289.
[31] S.P. Kounaves, D. Wen, P.Hallock, G. T. Kovacs, C. W. Storment, *Anal. Chem.* **1994**, *66*, 418.
[32] R.J. Reay, A.F. Flannery, C.W. Storment, S.P. Kounaves, G.T.A. Kovacs, *Sens. Actuators B* **1996**, *B34*, 450
[33] J.J. O'Dea, J. Osteryoung, in *Electroanalytical Chemistry*, Vol 14. (Ed: A.J. Bard), Marcel Dekker, New York **1986**, p. 209.
[34] J. Herdan, R. Feeney, S.P. Kounaves, G.T. Kovacs, C.W. Storment, B. Darling, *Env. Sci. & Tech.* **1998**, *32*, 131
[35] E.P. Gil, P. Ostapczuk, *Anal. Chim. Acta* **1994**, *293*, 55.
[36] J. Wang, J. Lu, *Anal. Chim. Acta* **1993**, *274*, 219.
[37] S.P. Kounaves, J.J. O'Dea, P. Chandresekhar, J. Osteryoung, *Anal. Chem*. **1987**, *59*, 386